RAPID COMMUNICATIONS

PHYSICAL REVIEW B VOLUME 49, NUMBER 15 15 APRIL 1994-I

ZnSe(100) surface: Atomic configurations, composition, and surface dipole

W. Chen and A. Kahn
Department of Electrical Engineering, Princeton University, Princeton, New Jersey 08544

P. Soukiassian
Commissariat a l'Energie Atomique, Centre d'Etudes de Saclay, 91191 Gif-sur-Yvette Cedex, France and Department of Physics, Northern Illinois University, Dekalb, Illinois 60115

P. S. Mangat
Department of Physics, Northern Illinois University, Dekalb, Illinois 60115

J. Gaines, C. Ponzoni, and D. Olego
Philips Laboratories, Briarcliff Manor, New York 10510
(Received 24 January 1994)

Chemical composition, core-level line shape, and electron affinity measurements are performed on the Se-terminated (2×1) and Zn-terminated $c(2\times2)$ ZnSe(100) surfaces. The (2×1) reconstruction corresponds to a complete monolayer of Se dimers with one filled dangling bond per surface atom. The $c(2\times2)$ reconstruction corresponds to a half-monolayer vacancy structure which leaves twofold-coordinated Zn atoms in the top layer. The 150-meV decrease in surface electron affinity at the $(2\times1)\rightarrow c(2\times2)$ transition is consistent with this model and results from a dipole induced by the charge transfer required to empty and fill all cation and anion dangling bonds on the $c(2\times2)$ surface, respectively.

II-VI compound semiconductors have attracted a great deal of attention since ZnSe-based blue-green laser diodes were first demonstrated.[1] Numerous studies have been devoted to the growth of ZnSe and related ternary and quaternary alloys, leading to substantial improvements in the crystalline and electronic quality of these materials.[2] Yet, there are so far only a few investigations of surfaces and interfaces of these materials, in spite of their obvious importance for understanding the chemistry and controlling the electronic properties of heterojunctions and contacts. Recent studies of tunability of heterojunction band lineups[3] and Schottky barrier heights on III-V semiconductors amply demonstrate the advantage of understanding surfaces and interfaces at the atomic scale.

Experimental studies of II-VI surfaces should also provide an important test of the basic principles which have been found to dominate the reconstruction of III-V surfaces. Accordingly, energy minimization via relaxation and dimerization, and surface autocompensation via charge transfer to fill (empty) all anion (cation) dangling bonds (DB) lead to a set of simple rules embodied by the electron counting rule[4,5] which has been used to explain III-V reconstructions and identify possible structures, i.e., configuration, stoichiometry, etc.

In this paper we present a multiple-technique investigation of ZnSe(100) which provides a self-consistent picture of the atomic geometry vs chemical environment of the surface species and work function across a range of Se vs Zn composition. We show that the Se-terminated (2×1) surface corresponds to a complete monolayer (ML) of anion dimers with fully occupied DB's, whereas the cation-terminated $c(2\times2)$ surface corresponds to a half-ML of nondimerized Zn atoms with empty DB's. We also show that these structures are compatible with the requirements imposed by the electron counting rule and explain the observed dipole-induced dependence of the work function. These results provide for the II-VI polar surfaces the necessary experimental verification of the validity of the rules previously developed for III-V surfaces.

ZnSe(100) layers (5000 Å thick) are grown by molecular-beam epitaxy (MBE). Doping levels are 2×10^{18} cm^{-3} for n-type ZnSe (Cl doped) and 5×10^{17} cm^{-3} for p-type ZnSe (N doped). The substrates are highly doped n- and p-type GaAs, respectively. The ZnSe surfaces are capped at low temperature ($T<0$ °C) in the growth chamber with a thick layer of Se for protection during ambient transfer. To prevent degradation of the Se cap, the samples are stored in low vacuum ($\sim10^{-3}$ Torr) before insertion into the analysis chamber. All subsequent experiments are done in ultrahigh vacuum ($P\leq10^{-10}$ Torr). The effectiveness of the Se capping method is demonstrated by the absence of any Zn photoemission signal from the capped layer and by the cleanliness of the decapped ZnSe surface.[6] The desorption of the bulk of the Se cap occurs at ~150 °C and is monitored through the appearance of the Zn photoemission signal. Subsequent decapping cycles at temperatures ranging up to 550 °C are performed by ramping slowly to the desired temperature, holding it constant for 1 min and cooling down to room temperature.

We use low-energy electron diffraction (LEED), ultraviolet photoemission spectroscopy (UPS; He discharge lamp), x-ray photoemission spectroscopy (XPS; 151.4 eV

$M\zeta$ line from a Zr anode) and contact potential difference (CPD) measurements (vibrating Kelvin probe) to follow reconstruction, band bending, surface composition, and work function, respectively. Soft-x-ray photoemission spectroscopy (SXPS) is performed at the Synchrotron Radiation Center of the University of Wisconsin. Zn 3*d* and Se 3*d* core-level spectra are collected using photon energies of 80 and 100 eV, respectively, which maximize surface sensitivity and signal intensity. At these energies, the combined resolution of the monochromator and analyzer is about 0.2 eV, as measured from the Fermi edge of a Au electrode.

When increasing the annealing temperature (T_A), we observe the (1×1) Se-saturated structure ($T_A \sim 200$ °C), the (2×1) Se-rich structure ($T_A \sim 300$ °C), and the $c(2\times2)$ Zn-rich structure ($T_A \sim 420$ °C). The (2×1) and $c(2\times2)$ patterns, photographed at 100 K (insets of Fig. 1) to reduce lattice vibrations, are sharp with a low background intensity, indicative of long-range surface atomic order.

The monotonic decrease of the XPS 3*d* core-level intensity ratio, I_{Se}/I_{Zn} (Fig. 1), is due to the desorption of the Se cap and of the top Se layer of the (100) surface with increasing temperature. In addition to the fact that both Se-rich (2×1) and Zn-rich $c(2\times2)$ reconstructions are observed for significant T_A windows, the I_{Se}/I_{Zn} curve is flat for the $c(2\times2)$ surface up to at least 530 °C which points out the stability of the Zn-rich reconstruction. The $c(2\times2)$ ratio is close to that obtained on the nonpolar (110) surface (arrow in Fig. 1) and indicates that the two surfaces have similar anion and cation relative densities. This is in contradiction with one of the models proposed for the $c(2\times2)$ surface based on the electron counting rule, namely, the full ML of Zn dimers.[4] On the other hand, it is consistent with the $\frac{1}{2}$-ML vacancy model already put forth on the basis of photoemission experiments.[7,8] The (110) surface and the $\frac{1}{2}$-ML vacancy (100) surface exhibit similar anion-to-cation relative densities in the top atomic planes.

The (110) calibration also helps evaluate the surface

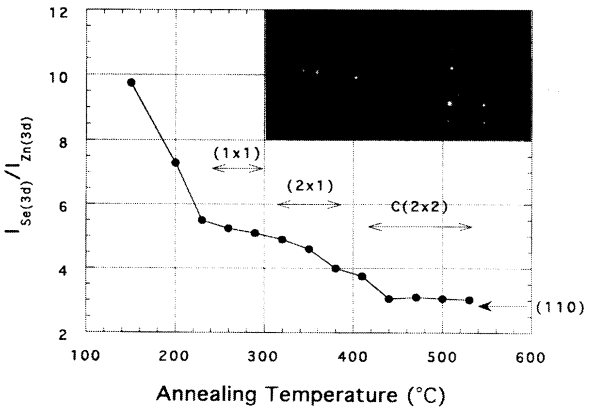

FIG. 1. Ratio of the Se 3*d* and Zn 3*d* core-level intensities measured as a function of decapping temperature. The photon energy is 151.4 eV. The corresponding structures observed by LEED are indicated. The inset includes the LEED patterns from the (2×1) and $c(2\times2)$ reconstructed surfaces.

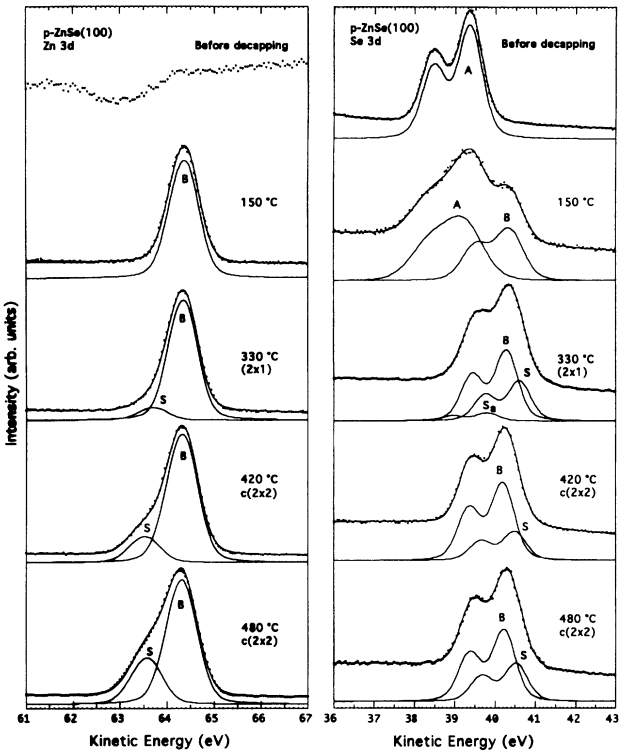

FIG. 2. Zn 3*d* and Se 3*d* core-level spectra as a function of annealing temperature. *B* and *S* represent the bulk and surface components for both species. *A* and S_a correspond to excess Se of the capping layer.

composition across the range of Se concentration. We find that the (1×1) structure corresponds to 2–3 ML of excess Se covering the Se-terminated lattice. The (1×1) structure is not understood, although it could result from disorder or from attenuation of diffraction features through the amorphous Se layer. The composition of the (2×1) surface obtained for $T_A = 330$ °C corresponds to a full ML of Se in the top layer. As a consequence, the reconstruction should correspond to a full ML of Se dimers.

The high-resolution SXPS Se 3*d* and Zn 3*d* core-level spectra (Fig. 2) are deconvolved into bulk and surface components using a least-square-fitting routine which simultaneously subtracts the integrated background and adjusts the core-level line shapes. The number of core-level components used in the fit is kept to a minimum, and stringent limits are placed on all parameters involved. The Se 3*d* parameters are obtained by fitting the data from the amorphous Se capping layer with one core-level component (top spectrum in Fig. 2). The Zn 3*d* parameters are obtained by fitting the data for the Se-saturated surface which does not have any surface Zn (150 °C spectrum in Fig. 2). All parameters are given in Table I.

For $T_A \sim 150$ °C, we still observe the presence of 2–3 ML's of Se remaining on the surface, as indicated by the excess Se component on the high-binding-energy side of the bulk Se peak. The shift is in the same direction as for amorphous As on GaAs.[9] A well-resolved single-

TABLE I. Fitting parameters for the Zn 3*d* and Se 3*d* core-level spectra for the clean ZnSe (100) surfaces. Binding energies (BE) are referencedto the energies of the bulk components (*B*). Positive (negative) BE shifts are toward higher (lower) BE's. All energies are in eV.

	Zn 3*d*	Se 3*d*
Spin-orbit splitting	0.31	0.85
Branching ratio	1.48	1.54
Gaussian width	0.54	0.56
Lorenzian width	0.15	0.20
BE shift of *S*	0.77	−0.32 (Se-rich), −0.30 (Zn-rich)

component Zn 3*d* spectrum is obtained from the same surface. A relatively small excess Se component (S_a, Fig. 2) remains visible up to $T_A \sim 300$ °C and vanishes beyond that point. The (2×1) reconstruction is then fully developed, and the Se peak exhibits a large surface component while the Zn peak is almost entirely accounted for by the bulk component. This is consistent with the (2×1) model of the surface terminated with a complete ML of dimerized Se. The surface Se component corresponds to Se in the dimers, and its intensity is relatively large because of the short escape depth of the photoemitted electrons. On the other hand, the Zn surface component should be negligible on a perfectly terminated surface. The residual component could correspond to surface defects which may have their origin in temperature inhomogeneities across the ZnSe surface during annealing cycles.

The situation is reversed on the $c(2\times2)$ surface, as indicated by the atomic configuration of Se-rich (2×1) and Zn-rich $c(2\times2)$ surfaces in Fig. 3. The $\frac{1}{2}$-ML vacancy model has $\frac{1}{2}$ ML of Zn exposed at the surface, leading to a large surface component (bottom two spectra in Fig. 2). The number of Se atoms with one DB is identical to that of the (2×1) surface, as shown by the similar ratios of the surface (*S*) and bulk (*B*) components in the 330 °C and 480 °C spectra. The 420 °C Se spectrum exhibits a peculiar decrease of the *S*/*B* ratio which could be related to the transition between the (2×1) and $c(2\times2)$ reconstructions.

Several additional points are also of interest. First, the shifts of the surface Zn and Se components toward higher and lower binding energies (Table I) with respect to their bulk components are parallel to those observed on III-V surfaces. They reflect an excess of electronic charge on the surface anion with respect to the bulk, and a deficiency on the surface cation. Second, the surface Se atoms experience slightly different chemical environments on the (2×1) and $c(2\times2)$ surfaces and therefore exhibit different surface core-level shifts. The difference, however, appears to be within the resolution of the curve-fitting procedure (~20 meV). Third, anion and cation core-level spectra corresponding to the (2×1) reconstruction exhibit only one surface component (Fig. 2), indicating that all surface atoms are chemically equivalent [unlike on GaAs(100)]. The same is true also for the $c(2\times2)$ reconstruction. This latter point supports a model of symmetric dimers for the Se-terminated surface.

The CPD measurements of work-function changes coupled with UPS measurements of band-bending changes show that the electron affinity (EA) of the ZnSe surface increases with the removal of the Se capping layer. The EA goes through a maximum for the (2×1) reconstruction, decreases by 150 meV for the $c(2\times2)$ reconstruction, and remains steady thereafter (Fig. 4). Here again, this evolution is qualitatively similar to that obtained on the GaAs(100) surface,[10] although the magnitude of the EA swing between the anion- and cation-rich surfaces is clearly smaller than in the III-V case.

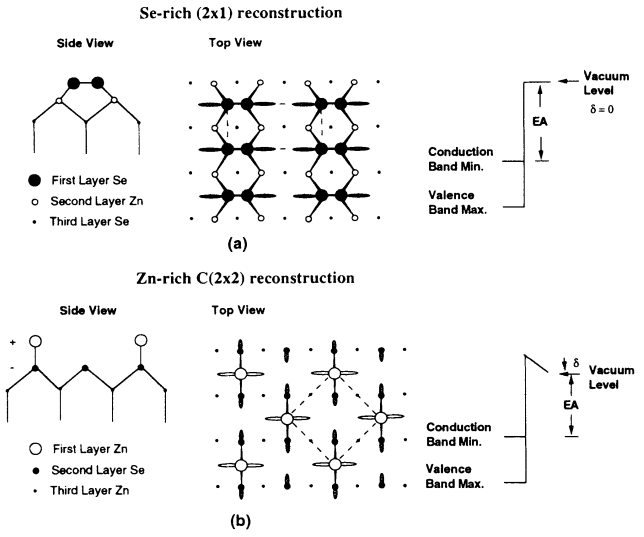

FIG. 3. Ball and stick models of the top three atomic layers of ZnSe(100) for the (a) (2×1) and (b) $c(2\times2)$ reconstructions. The dashed lines outline the unit cells. Filled and empty dangling bonds are represented. The right-hand part shows the surface energy diagram with the change in electron affinity (EA) due to the charge-exchange-induced surface dipole (δ). δ=0 for the (2×1) surface.

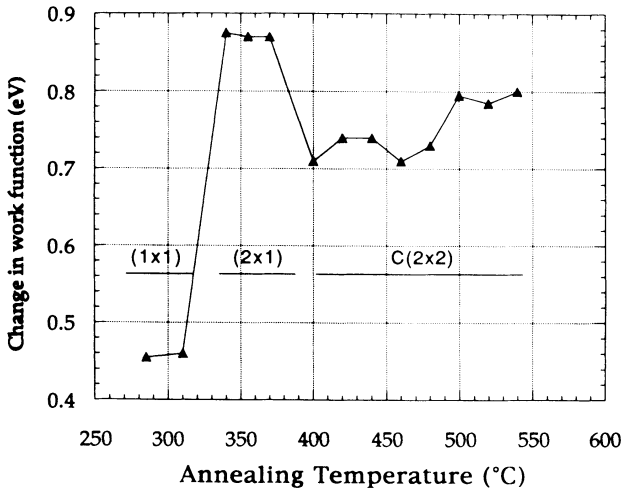

FIG. 4. Variation of the work function measured by CPD as a function of annealing temperature. The accuracy on each measurement is 20 meV.

The initial increase in EA is due to the progressive removal of the amorphous Se layer and is of little interest for the present study. The important part of the EA swing occurs between the (2×1) and $c(2\times2)$ structures and reflects a *change in surface dipole* caused by a change in the DB occupancy in the top two layers. According to the electron counting rule, Se with six valence electrons contributes on average 1.5 electrons to each tetrahedral bond, while Zn with two valence electrons contributes $\frac{1}{2}$ electron to each bond. On the (2×1) surface, each Se uses therefore three electrons for bonding to two second-layer Zn atoms, one electron in the dimer bond and is thus left with exactly two electrons to fill its DB. The ML Se-dimer configuration fits therefore precisely the number of available valence electrons. As a result, the surface Se is neutral, the Se DB is filled, and there is no surface dipole. The $c(2\times2)$ vacancy structure, on the other hand, is such that each unit cell has two Zn DB's in the top layer and two Se DB's in the second layer (Fig. 3). According to the electron counting rule, each Zn DB carries $\frac{1}{2}$ electron, whereas each Se DB has only $\frac{3}{2}$ electron. Autocompensation takes place through transfer of $\frac{1}{2}$ electron from each Zn DB to each Se DB, leading to empty and filled cation and anion DB's, respectively. This charge transfer sets up a dipole (δ in Fig. 3) which lowers the EA (Fig. 4). The EA swing is weaker than on GaAs for two reasons. First, the anion-rich ZnSe surface does not exhibit a dipole, whereas the III-V counterpart does (charge transfer with opposite sign for the anion- and cation-terminated surfaces). Second, the charge transfer is $\sim\frac{3}{4}$ electron/DB in the III-V case, and only $\frac{1}{2}$ electron/DB in the present case. The EA variation with reconstruction, however, appears to be a very general feature of polar surface, and is entirely consistent with the structural model inferred from LEED, SXPS, and the electron counting rule.

In conclusion, we have shown that the (100) surface of ZnSe obtained by MBE and Se decapping exhibits two reconstructions depending on the annealing temperature. The (2×1) Se-rich reconstruction corresponds to a full monolayer of symmetric anion dimers whereas the $c(2\times2)$ Zn-rich reconstruction corresponds to a half-monolayer of nondimerized cations. The latter is a clear departure from the dimer-based reconstructions generally observed on cation-terminated (100) III-V surfaces, in particular GaAs. The cation-to-anion charge transfer necessary to satisfy the requirement of DB saturation on the $c(2\times2)$ surface introduces a surface dipole which explains the decrease observed in the electron affinity of the surface.

This work was supported by the National Science Foundation under Contract No. DMR-90-18521 through Princeton University, and Contract No. DMR-92-23710 through Northern Illinois University. This work is based upon research conducted in part at the Synchrotron Radiation Center of the University of Wisconsin in Madison, which is supported by the National Science Foundation under Contract No. DMR-92-12652.

[1]M. A. Haase, J. Qiu, J. M. DePuydt, and H. Cheng, Appl. Phys. Lett. **59**, 1272 (1991).

[2]See, for example, Proceedings of the Sixth International Conference on II-VI Compounds and Related Optoelectronic Materials, Rhode Island, 1993, edited by A. Nurmikko, T. Yao, and R. Ruth [J. Cryst. Growth (to be published)].

[3]A. Franciosi, L. Sorba, G. Bratina, and G. Biasiol, J. Vac. Sci. Technol. B **11**, 1629 (1993).

[4]M. D. Pashley, Phys. Rev. B **40**, 10 481 (1989).

[5]W. A. Harrison, J. Vac. Sci. Technol. **16**, 1492 (1979).

[6]W. Chen, A. Kahn, P. S. Mangat, P. Soukiasian, J. Gaines, C. Ponzoni, and D. Olego, J. Vac. Sci. Technol. (to be published).

[7]M. Vos, F. Xu, Steven G. Anderson, J. Weaver, and H. Cheng, Phys. Rev. B **39**, 10 744 (1989).

[8]H. H. Farrell, M. C. Tamargo, and S. M. Shibli, J. Vac. Sci. Technol. B **8**, 884 (1990).

[9]G. Le Lay, D. Mao, A. Kahn, Y. Hwu, and G. Margaritondo, Phys. Rev. B **43**, 14 301 (1991).

[10]W. Chen, M. Dumas, D. Mao, and A. Kahn, J. Vac. Sci. Technol. B **10**, 1886 (1992).

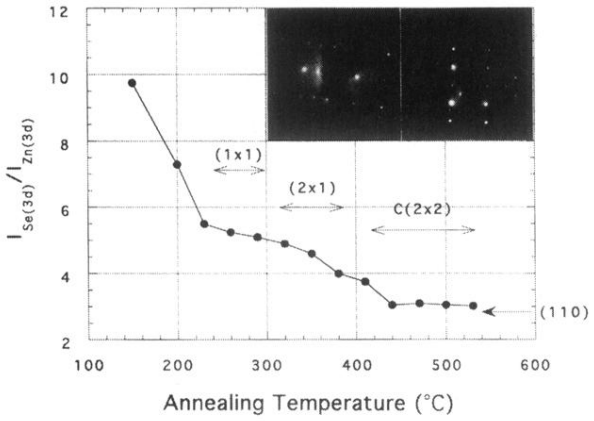

FIG. 1. Ratio of the Se 3*d* and Zn 3*d* core-level intensities measured as a function of decapping temperature. The photon energy is 151.4 eV. The corresponding structures observed by LEED are indicated. The inset includes the LEED patterns from the (2×1) and $c(2\times2)$ reconstructed surfaces.